Performance assessment of natural gas and biogas fueled molten carbonate fuel cells in carbon capture configuration

Linda Barelli [a], Gianni Bidini [a], Stefano Campanari [b], Gabriele Discepoli [a, *], Maurizio Spinelli [b]

[a] *Università degli Studi di Perugia, Department of Engineering, Via Duranti 67, 06125 Perugia, Italy*
[b] *Politecnico di Milano, Department of Energy, Group of Energy Conversion Systems, Via Lambruschini 4, 20156 Milano, Italy*

The ability of MCFCs as carbon dioxide concentrator is an alternative solution among the carbon capture and storage (*CCS*) technologies to reduce the CO_2 emission of an existing plant, providing energy instead of implying penalties. Moreover, the fuel flexibility exhibited by MCFCs increases the interest on such a solution.

This paper provides the performance characterization of MCFCs operated in CCS configuration and fed with either natural gas or biogas. Experimental results are referred to a base CCS unit constituted by a MCFC stack fed from a reformer and integrated with an oxycombustor. A comparative analysis is carried out to evaluate the effect of fuel composition on energy efficiency and CO_2 capture performance.

A higher CO_2 removal ability is revealed for the natural feeding case, bringing to a significant reduction in MCFC total area (−11.5%) and to an increase in produced net power (+13%). Moreover, the separated CO_2 results in 89% (natural gas) and 86.5% (biogas) of the CO_2 globally delivered by the CCS base unit. Further investigation will be carried out to provide a comprehensive assessment of the different solu-tions eco-efficiency considering also the biogas source and availability.

Keywords:
Molten carbonate fuel cell
Carbon capture
Biogas
Natural gas
Experimental

1. Introduction

During the last decades, the growing concern about global warming and the simultaneous awareness of fossil fuels scarcity have pushed scientific and industrial research towards innovative solutions in the field of carbon capture and sequestration (CCS) and renewable energy. So far, strong efforts have been done in multi-disciplinary contests (e.g. experimental and numerical studies focused on power systems design and optimization) to find out the best technical alternatives for facing the increasing energy demand and the urgent topics related to environmental sustainability and energy efficiency. Several studies have shown how these critical topics could find a promising solution in Molten Carbonate Fuel Cell (MCFC) technology, thanks to its excellent efficiency and intrinsic operation.

Fuel cells represent one of the most efficient devices for direct energy conversion. Amongst them, MCFCs can be operated flexibly with different fuel compositions and can also be exploited as car-bon dioxide concentrators. Indeed, the electrochemical process that takes place within MCFCs (Eqs. (1) and (2)) involves the migration of CO_2 molecules from the cathode to the anode of the fuel cell (FC). This process plays a key role in the FC power generation and can be useful for separating a pure CO_2 stream from some kind of exhausts

* Corresponding author.
E-*mail address:* gabriele.discepoli@unipg.it (G. Discepoli).

Published Journal Article available at: http://dx.doi.org/10.1016/j.jpowsour.2016.04.071

gases fed to the cathode side, following a concept already investigated in several simulation [1–5] and experimental [6–9] works, for large and small scale applications. Moreover, on the anode side, the combination of high operating temperature (~650 °C) and catalytic metals within FC layers (Ni-based) fosters the internal fuel reforming, enabling the fuel cell operation with natural gas, biogas or other gaseous fuels directly.

Fuel flexibility is widely acknowledged as one of the most attractive features of these devices and gives way to the utilization of renewable and other unconventional fuels. This solution has been widely discussed in literature where information about some demonstration pilot and industrial FC modules are available, for instance the thermal integration of MCFCs and anaerobic digesters to produce heat and power in waste water treatment stations facilities [10] wherein a moderate voltage loss with respect to pure natural gas operation must be acknowledged owing to the mixture of biogas and natural gas that is supplied to the anode [11].

Despite this efficiency reduction, which is naturally associated to the different fuel composition, several publications recognize the enormous synergy potential between fuel cells and biogas systems, considering the wide deployment of biogas production facilities and the possibility of providing a de-centralized power production by means of a sustainable and clean primary energy supply [12]. One of the critical point of this joint development is the design of a proper and cost-effective fuel processing system. Biogas clean-up processes involve the installation of ultra-efficient purification technologies, for reasons associated to the severe poisoning effect of H_2S, mercaptane, siloxane and other minor trace gases on MCFC catalytic materials [12–15]. In particular, sulfur traces are a well recognized issue for high temperature fuel cells, whose performances and durability are strongly affected by the poisoning mechanisms that arise on the anode and cathode surfaces (nickel sulphide formation), and also within the electrolyte (sulphate formation) [16]. For this reason the tolerance on H_2S (on the anode side) and SO_2 (at the cathode) is commonly assumed to be very close to 1 *ppm* [17–19].

Small size fuel cell power plant fed by natural gas/biogas have already been considered a promising solution for CO_2 separation when integrated in a wastewater treatment facility [1]. In this framework, the unusual working conditions that arise from both CCS assessment (high CO_2 utilization factors) and utilization of alternative fuels (different H/C ratios with respect to NG), require a deep investigation on MCFC behavior inasmuch as these could meet operational limits on waste heat management or critical overpotential losses (due to high U_{CO_2}). In this work, the particular operative conditions of this kind of power plants is considered which could influence the system design and plant performances in terms of electric and CO_2 capture efficiencies; these aspects are herein evaluated through comparative analysis.

Natural gas and biogas feeding options are analyzed and compared in Ref. [20] but only for MCFC installations in wastewater treatment facilities with trigeneration scopes. Nevertheless, the study does not consider the CCS application and is based only on modeling results. Other authors approach the integration of wastewater treatment facilities with MCFC units [21]; not including CCS application and considering biogas utilization only; unfortunately, this work does not rely on experimental data. MCFCs powered by biogas are further investigated in Ref. [22] through model simulations considering both CCS and trigeneration scopes. Comparative assessments based on experimental data and relative to the exploitation of biogas and city gas are finally provided in Refs. [23], but they deal with a different application based on a MCFC/micro gas turbine hybrid plant which does not include CCS.

This literature review therefore evidences the lack of studies on biogas-fed MCFC based on a specific experimental investigation. The main contribution of the present study is thus to approach a comparative analysis based on experimental tests performed at lab-scale on MCFCs operated in CCS configuration and fed with either natural gas or biogas. Moreover, these tests were carried out with cathodic streams reproducing real exhaust gases from conventional internal combustion engines.

The specific target of the present work is hence to characterize and compare the utilization of MCFCs in CCS application with natural gas or bio gas fuels. In order to obtain a generalized result, this analysis is performed on a reference base CCS unit installed downstream of a reciprocating internal combustion engine (ICE). The fuel cell CCS subsystem is in practice constituted by a MCFC stack directly fed from a reformer and integrated with an oxy-combustor and ASU assembly (*Air Separator Unit*). A comparative analysis is carried out to evaluate the effect of fuel composition on energy efficiency and CO_2 capture performance of the considered base CCS unit, as well as on its sizing. Furthermore, improvements that could be attained in terms of CO_2 performance under particular operating conditions and potential reductions of investments costs are investigated for the operation on natural gas, biogas and specific fuel blends reported in Ref. [1] as result of system optimization.

From a practical standpoint, all the evaluations are based on results from preliminary experimental activities aimed at investigating (through the determination of polarization curves) the fuel cell behavior in CCS applications. Overall, three different reformed fuels (obtained by a proper combination of natural gas and biogas) and three different cathode gases, all derived from assessments relative to plant layouts discussed in Refs. [1], are considered for the experimental activity whose test campaign is then scheduled to fully characterize the MCFC behavior in terms of H_2, O_2 and CO_2 utilization factors, resulting in the functional relations between electric efficiency, CO_2 capture rate and current density. These laboratory simulations are then exploited for a first theoretical design of the base CCS unit to be ideally integrated as a carbon concentrator in a sewage treatment facility.

Finally, this work has been further extended with the techno-economic simulation of the most interesting case studies among those initially investigated. The techno-economic evaluations aim to identify the most profitable MCFC feeding conditions and, therefore, to optimize plants layouts previously considered for the retrofitting of a wastewater treatment plant equipped with reciprocating engines. Specifically, techno-economic evaluations are approached by assuming two alternative design criteria (constant installed MCFC electric power or constant exhausts flow rate to be processed), both assessed on the basis of the most promising configurations emerged from the experimental activity.

The main findings are the ability of the CCS unit (MCFC + oxycombustor) to store 89% and 86% of the treated carbon dioxide for the natural gas and biogas fueled systems respectively.
The former solution produces 0.485 $kWh \cdot kg_{CO_2}^{-1}$ (kWh for kilogram of stored CO_2) whilst the latter reaches 0.41 $kWh \cdot kg_{CO_2}^{-1}$.

Moreover, the study confirms the extreme importance of MCFC capital cost on the competitiveness of this type of installations, which enables the efficient capture of CO_2 even if only after a wide deployment of the technology that ensures mass production and hence lower costs; otherwise the solution is technically feasible but not economically appealing.

2. Carbon capture from an existing plant

2.1. MCFC: operating principle

MCFCs are DC power units that exploit the following electrochemical reactions to generate current (even if other secondary reactions may contribute to generate electricity):

$$\frac{1}{2}O_2 + CO_2 + 2^- \rightarrow CO_3^= \quad (cathode) \tag{1}$$

$$H_2 + CO_3^= \rightarrow H_2O + CO_2 + 2e^- \quad (anode) \tag{2}$$

$$H_2 + \frac{1}{2}O_2 + CO_2 \rightarrow H_2O + CO_2 \quad (total) \tag{3}$$

The ability of MCFCs to convey CO_2 from the cathode to the anode, via $CO_3^=$ ion migration across the electrolyte (Fig. 1), characterizes this fuel cell and enables its utilization as a carbon dioxide concentrator [24,7]. Also the Water Gas Shift (*WGS*) reaction, which can reach equilibrium quite fast in the investigated operative conditions (see Section 3.2), has an effect on the anode off-gas composition [25]:

$$CO + H_2O \rightarrow CO_2 + H_2 \quad (water\ gas\ shift) \tag{4}$$

Table 1
Composition of anodic mixtures for the three cases proposed.

Fuel molar compositions	*ng*	*bio*	*biopt*
X_{CO}	7.92	5.51	5.98
X_{CO_2}	8.84	13.32	12.44
X_{H_2}	58.48	42.05	45.36
X_{H_2O}	24.49	38.13	35.4
X_{N_2}	0.27	0.99	0.82
Total Flow [$ml\ min^{-1}\ cm^{-2}$]	2.65	3.23	3.10
Dry Flow [$ml\ min^{-1}\ cm^{-2}$]	2.0	2.0	2.0

Table 2
Composition of cathodic mixtures for the three cases considered.

Oxidant molar compositions	*base*	*enr*	*copt*
X_{CO_2}	12.3	9.1	7.3
X_{H_2O}	15.5	11.5	9.9
X_{O_2}	2.8	7.4	13.0
X_{N_2}	69.5	71.9	69.8
Total Flow [$ml\ min^{-1}\ cm^{-2}$]	15.16	14.45	14.21
Dry Flow [$ml\ min^{-1}\ cm^{-2}$]	12.8	12.8	12.8

2.2. MCFC-CCS base unit

In the present paper, it is assumed to treat exhaust gases from an existing ICE group by means of a unit, namely *base CCS unit*, constituted by a MCFC stack integrated with an oxycombustor-ASU and directly fed through a reformer. The base CCS unit is installed downstream the ICE plant and fueled by natural gas or biogas. Fig. 1 shows a schematic representation of CO_2 streams within the CCS base unit. Cathode inlet stands for the exhaust gases to be processed while $CO_{2\,emitted}$ is the residual carbon dioxide that is still present in the process gas at the cathode outlet. The composition and temperature at anode inlet are determined by the different MCFC feeding strategies investigated herein. This information is presented in Tables 1 and 2 where the anodic and cathodic feeding conditions considered in the comparative analysis are presented; in these tables, $CO_{2\,fuel}$ and $CO_{2\,exhaust}$ are the corresponding CO_2 streams entering the MCFC on the anode and cathode sides respectively. Only in the *biopt-copt* case (see Tables 1 and 2), the carbon dioxide stream at cathode inlet ($CO_{2\,inlet}^{cath}$) differs from $CO_{2\,exhaust}$ as a result of the recirculation loop added to the stack. This recirculation loop also implies that the carbon dioxide stream at cathode outlet ($CO_{2\,out}^{cath}$) differs from $CO_{2\,emitted}$. $CO_{2\,rem}$ is the internal CO_2 stream transferred by the cell from cathode to anode, strictly related to the CO_2 concentrator capability exhibited by the MCFC stack. Consequently, $CO_{2\,out}^{an}$ is the carbon dioxide stream resulting from the sum of $CO_{2\,rem}$ and $CO_{2\,fuel}$; $CO_{2\,out}^{an}$ coincides with $CO_{2\,in}^{oxy}$ in all cases except for *biopt-copt* similarly to the cathode side as consequence of the second recirculation loop. Since the anodic off-gas still contains unreacted species (in the following H_2 and CO are considered), the oxycombustor is needed to allow for CO_2 separation through water condensation. Therefore, $CO_{2\,storage}$, determined as the sum of $CO_{2\,in}^{oxy}$ and the carbon dioxide produced by oxycombustion CO_2^{CO}, is the carbon dioxide which can be separated and delivered to subsequent treatments (e.g. compression, liquefaction).

2.3. Anodic conditions

In the experimental activity performed in order to assess the MCFC behavior, three different anodic mixtures with the same overall dry volumetric flow rate were considered (Table 1). The first fuel (*ng*) is a typical reformate gas (steam reformed natural gas) constituted by carbon monoxide and dioxide, hydrogen, water and traces of nitrogen. The second composition proposed (*bio*) is a reformate gas but, in this case, from a typical anaerobic digestion biogas; this anodic gas is a mixture containing the same species but

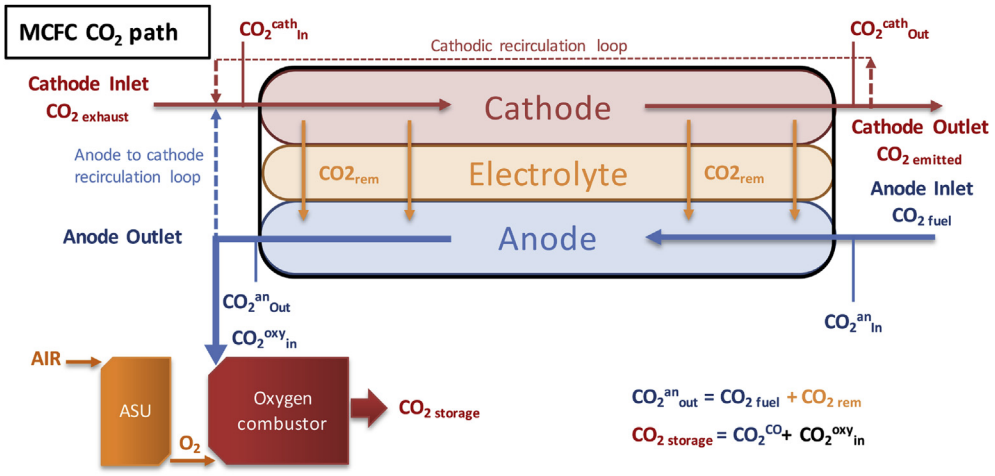

Fig. 1. MCFC working principle scheme, under *CCS* conditions, as implemented in the CCS base unit under study.

in a different proportion. Finally, the third mixture (*biopt*) derives from same biogas but its composition relates to a particular plant optimization as discussed in Ref. [1]. For the sake of simplicity, full hydrocarbon conversion in the reformer is assumed in all cases.

Given that this work is aimed at characterizing the thermo-electric and economic performances of MCFC applied to CCS both for natural gas and biogas operation, fuel processing is simply constituted by a reforming unit downstream a clean-up section. This is the reason why the third mixture was considered, since it has intermediate features between natural gas and biogas and hence allows for a better characterization of the MCFC behavior when fed by natural gas or biogas. In summary, three fuels are considered:

1. reformed natural gas (*ng*);
2. reformed biogas (*bio*);
3. bio-optimized gas (*biopt*).

For each fuel mixture Fig. 2A highlights the fuel utilization factor

calculated, referred to the equivalent hydrogen flow rate H_2^{eq} (Eq. (5)), as a function of current density. H_2^{eq} is defined as follows:

$$H_2^{eq} = m_{H_2} + m_{CO} + 4m_{CH_4} \tag{5}$$

where m_{H_2}, m_{CO} and m_{CH_4} are, respectively, the hydrogen, carbon monoxide and methane molar flow rates in the fuel stream. m_{CH_4} is equal to zero in all the cases considered here.

The trend obtained for the *biopt* mixture lies between the others, even if the two biogas-derived compositions are quite similar. The *ng* fuel exploitation trend, instead, is far from the *biogas* case which is an important feature with an important effect on efficiency. This is discussed below.

2.4. Cathodic conditions

In order to characterize the MCFC performance in a CCS application, the composition of the cathode inlet stream is similar to the exhaust gases of reciprocating engine operating on biogas; i.e. combustion gases of biogas and air in stoichiometric conditions. Specifically, aiming to better highlight and characterize the MCFC behavior, three different cases are investigated (Table 2):

1. exhaust gases “as is” (*base*);
2. exhaust gases enriched with air to provide suitable oxygen content without diluting the mixture too much, thus keeping the carbon dioxide content over 9% (*enr*);
3. the cathodic mixture indicated in Ref. [1] (*copt*) relative to *biopt*.

Table 2 summarizes the main features of the cathodic mixtures, whose dry volume flow rate is the same for all the cases under study, and Fig. 2B presents the trends of oxygen utilization factor (U_{ox}), showing that the composition of the cathodic mixture varies as a function of current density. Also the trend of ratio P_{O_2}/P_{CO_2} of partial pressure is depicted in this figure.

Finally, the trends of carbon dioxide utilization factor (U_{CO_2}) when varying the current density are plotted in Fig. 2C for all the investigated cases. These influence of all these parameters on voltage, power and efficiency are discussed in Section 4.

3. Experimental

3.1. Setup and methodology

The entire test campaign was performed by Fuel Cell Laboratory staff at the University of Perugia. Specifically, tests were carried out on individual molten carbonate cells with dimensions 8.9 × 8.9 *cm* (approximate surface area 80 cm^2) supplied by FCES (*FuelCell Energie Solutions GmbH*). The electrodes are Nickel based and the electrolyte is a typical lithium carbonate and potassium carbonate mixture. Further details are not available because of confidentiality. The fuel cell is sandwiched between two current collectors and included in the anodic and cathodic frames (Fig. 3) which supply the gas, expel the exhaust gases and drain the electric current collected. The MCFC works under a mechanic load of 2.2 bar produced by a hydraulic piston to avoid gas leakage across the cell borders. The test facility lay-out is already described in details in Ref. [26]. The main instruments are: Agilent Technologies DC Electronic Loads N3304A, using remote sensing input for the monitoring of current (resolution: 0.1 *mA*; accuracy:±0.05% + 5 *mA*) and cell voltage (resolution: 0.1 *mV*; accuracy:±0.05% + 3 *mV*) directly at the electrodes; Brooks 5850E Digital Mass Flow Controllers (±0.7% of rate and ±0.2% F.S.) selected for their high accuracy. All the instruments are managed by a software installed in a remote PC.

The test bench operates in current mode. Each point of the current density-voltage (*I-V*) curve is measured at 1 Hz intervals for at least 10 min after the fuel cell voltage is stabilized. The final value for each parameter is obtained by averaging all collected data during this stable phase.

The experimental activity is aimed to determine the MCFC performance under different feeding (anodic and cathodic) and other operative conditions. The thermal balance management was not included in the study because not relevant in tests on single cells. These tests were performed because they allows a great flexibility with respect to reagents type and voltage-current conditions but, on the other hand, they are usually led at constant

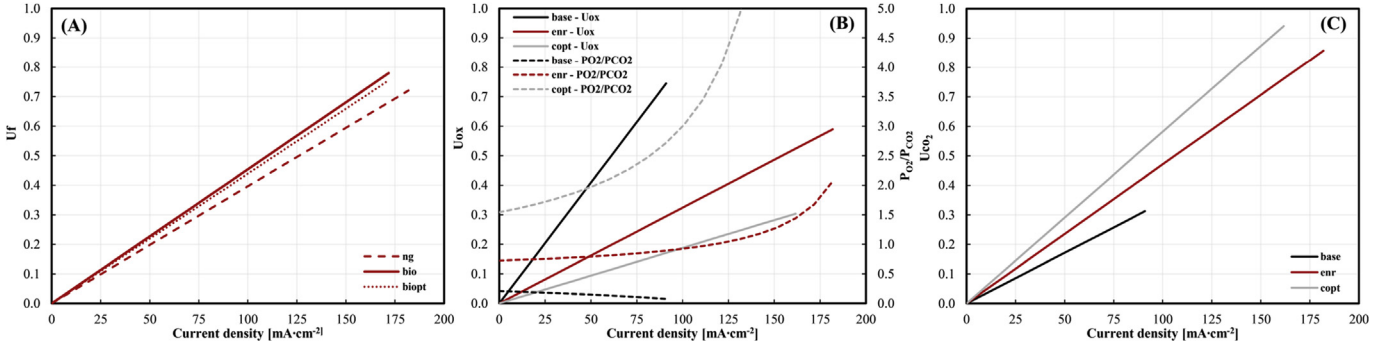

Fig. 2. (A) U_f trend for the three different anodic compositions; (B) trends of U_{ox} and P_{O_2}/P_{CO_2} as function of current density for all cathodic mixtures; (C) trend of U_{CO_2} as a function of current density for all cathodic mixtures.

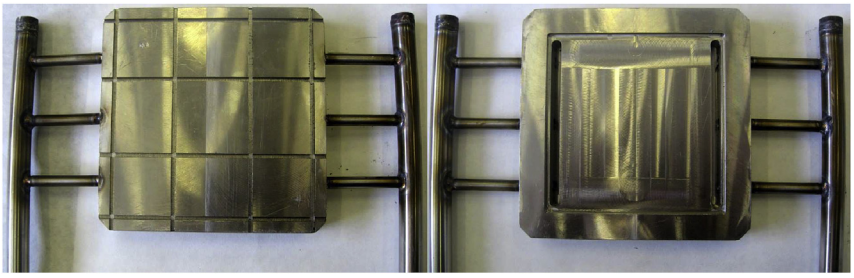

Fig. 3. Internal and external views of the MCFC frames: this is a classical lay-out to collect current and supply gas to the fuel cell.

temperature, imposed by the test facility. Consequently, in the thermal balance the heat contribution provided by the oven in which the single cell is located is predominant in relation to the thermal behavior of the cell. This approach is usually chosen because it allows repeatable results and highlights the effect of specific operative parameters (anodic/cathodic mixtures, current density, fuel utilization, carbon dioxide utilization and O_2/CO_2 partial pressure ratio) on cell performance without any temperature influence. Vice versa, at full size system level, the heat production and management will demand additional analysis for a more realistic assessment, also depending on the system lay-out, e.g. the possible presence of an integrated reforming system that takes part to the heat exchanges inside the stack.

3.2. Test campaign and operative condition description

In order to deeply understand MCFC behavior, a full set of nine operative cases combining the three anodic compositions with all three cathodic mixtures was considered. Each case was experimentally characterized by determining its corresponding *I-V* polarization curve which was determined by measuring the fuel cell voltage for increasing current density in incremental steps of 10 $mA\ cm^{-2}$, from *OCV* (Open Circuit Voltage) to the maximum current allowed. Each operating point (i.e. current) was held for at least 10 min in steady conditions during which fuel cell voltage was sampled at 1 *Hz* frequency. The data gathered were recovered and processed afterwards.

All tests were performed at 650 $^{\circ}C$ whilst the anodic and cathodic mixtures were supplied to the cell at room temperature and pressure. Just after the mixtures humidification (throughout bubblers), temperature was kept over 80 $^{\circ}C$ to avoid the formation of water drops due to water condensation given that the resulting discontinuous evaporation would make the fuel cell unstable. The test campaign was completed in about 96 h, a time interval sufficiently narrow to consider the single MCFC performance stable in the whole campaign.

4. Results

4.1. Energy performances

I-V curves, are plotted in Fig. 4A, where the color and marker codes identify the various cathodic compositions and anodic mixtures respectively. A first general remark is that the *I-V* curve trend seems to be dominated by the cathodic mixture whereas the anodic inlet streams have a lower order influence: the *base* cases reach poor performance, the *copt* cases correspond to very tied curves while in the *enr* cases higher power outputs are reached.

For the *enr* and *copt* cases the limiting factor is the cathodic carbon dioxide. In particular the great CO_2 exploitation (U_{CO_2} curves as visible in Fig. 2C) prevents *copt* curves to reach higher current densities (almost 95% at 160 $mA\ cm^{-2}$). On the other hand, voltage of *base* case drops quickly due to poor oxygen content in the cathodic mixture. In fact, in this case U_{ox} reaches 74% at 90 $mA\ cm^2$ (Fig. 2B) with an oxygen concentration in the cathodic exhaust of 1.7% and, consequently, a P_{O_2}/P_{CO_2} ratio steadily under 0.25 (black dotted line), significantly lower than the minimum threshold fixed for typical working conditions [7]. This behavior implies the need of an air enrichment of the internal combustion engine exhaust, before accessing the cathode, as done in cases *enr* and *copt*. This fact makes *base* cathodic compositions not interesting for CCS appli-cation; therefore, in the following it is no longer taken into account for purposes of the present study.

The reason why *I-V* curves, obtained with cathodic *copt* varying the anodic feeding conditions, are so tight each others, probably should be searched on the higher U_{CO_2} factor (Fig. 2C). In fact, *copt* shows less oxygen exploitation respect to *base* and *enr* cathodic compositions. This is particularly evident observing the trend of P_{O_2}/P_{CO_2} ratio, which assumes, for *copt* case, values significantly higher than the other cases. The *enr* case, instead, characterized by lower values of P_{O_2}/P_{CO_2} ratio (but always greater than the minimum threshold fixed for typical working conditions in (7]), is useful to highlight the effect of anodic feeding mixtures on *I-V* curves. In particular, as expected, the obtained voltage increases with the LHV of the mixture (*CO* and H_2 content), e.g. at 160 $mA\ cm^{-2}$, the voltage is 574 *mV* (*bio*), 592 *mV* (*biopt*) and 636 *mV* (*ng*) with fuel con-centration of 1.54, 1.59 and 1.76 $ml\ min^{-1}\ cm^{-2}$ respectively. In particular, *enr* curve with *ng* fuel gains over the corresponding *bio* one (red diamonds and squares) up to almost 15%, while this dif-ference expires in the cases of cathodic compositions *copt*, for what discussed above, and *base* (in this last case for the pure oxygen content).

Regarding efficiency (Fig. 4B), for fixed current densities, the biogas-like fuels reach higher electric efficiency values due to the greater fuel exploitation (Fig. 2A). This occurs for all cathodic mixtures, although the maximum absolute values are close for *enr* and *copt* curves, with the exception of the *ng-copt* case. In particular, it seems that the maximum reachable efficiency is depending from the cathode and the *enr* case shows the best performance. Furthermore, it is also evident that relative to energy performance (*V* and η_e), *biopt* curves fall between *ng* and *bio* ones, very tight to the latter. In conclusion, it can be highlighted how the efficiency is markedly depending from the fuel kind up to high current density, where the cathode becomes more affecting: the high cathodic gas species exploitation (carbon dioxide for *enr* and *copt* cases, oxygen for *base*) limits the fuel cell to reach higher current densities, actually characterized by greater fuel utilization and the customary high electric efficiency performance.

4.2. Carbon capture performances

Beyond the carbon dioxide separated from the cathode gas inlet

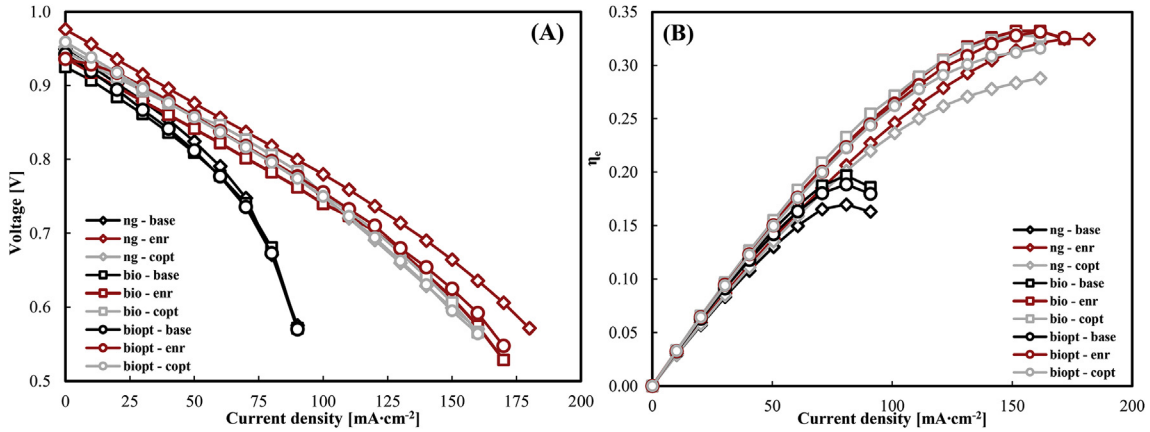

Fig. 4. (A) MCFC *I-V* polarization curves for the 9 different cases; (B) electric efficiency curves for all the tested compositions.

($CO_{2\ rem}$ as in Fig. 1), at anodic outlet the MCFC will also collect the carbon dioxide coming from the particular used fuel ($CO_{2\ fuel}$), i.e. carbon dioxide inherently contained in the fuel (biogas) and the one produced by the reforming of natural gas or biogas via water gas shift reaction (*WGS*). This CO_2 contribution is characteristic of the used fuel and rather effects the overall quantity of the carbon dioxide flow concentrated at the anode side. Due to that, even if the natural gas operation mode reaches higher current densities, meaning higher quantity of CO_2 separated from the cathodic flow ($CO_{2\ rem}$), using biogas as a fuel brings about a higher $CO_{2\ fuel}$ (as evident from Table 1, biogas supplies almost 46% additional CO_2 with respect to natural gas), finally reaching a higher captured CO_2 fraction ($CO^{an}_{2\ out}$, depicted in Fig. 5 as percentage of the overall carbon dioxide in input to the MCFC) compared with the results obtained for natural gas.

In the following, the impact of *ng* and *bio* fuel on carbon capture performance is discussed, also with reference to *enr* and *copt* cathodic operative conditions.

As previously seen, mixtures *biopt* and *copt*, relating to a particular plant optimization as discussed in Refs. [1], do not add particular value from an energetic point of view: *biopt* curves do not distance the *bio* curves in voltage and efficiency (but quite better than *ng* on the efficiency) and *copt* curves were substantially below the corresponding obtained in *enr*.

On the other hand, Fig. 5 (gray lines) highlights the benefit obtainable in terms of capture performances specifically for *copt* cathodic condition, respectively for *bio-copt* and *ng-copt*: about 95% and 94% of the overall CO_2 is collected at the anodic off-gases at 160 $mA\ cm^{-2}$, while 82% and 80% is the target achieved at same current density in case of cathodic mixture *enr*. In fact, the U_{CO_2} curve for the *copt* case is considerably more steep (Fig. 2C). This is possible because in *copt* the oxidant mixture is better exploited by working with the highest oxygen excess ($U_{ox} < 0.3$, Fig. 2B).

At fixed current densities, the energy produced for kilogram of captured CO_2 significantly depends on the particular used fuel (i.e. the voltage), since the curves with the same fuel are very tight (Fig. 6). Consequently the *ng* feeding condition is favored. Furthermore, *ng-curves* show analogues trends, increasing quickly at low current densities to slightly decrease for high value of the current. This behavior is due to the linear dependence of $CO^{an}_{2\ out}$ from current density, while produced energy is proportional to power. Therefore, when power reaches its plateau, $CO^{an}_{2\ out}$ is still growing and then the energy per *kg* of CO_2 captured falls down. Moreover, *ng-curves* showed a range of values between 0.590 and 0.470 $kWh \cdot kg^{-1}_{CO_2}$ at the highest currents, while the maximum value of 0.710 $kWh \cdot kg^{-1}_{CO_2}$ is reached in the case of *ng-enr* composition,

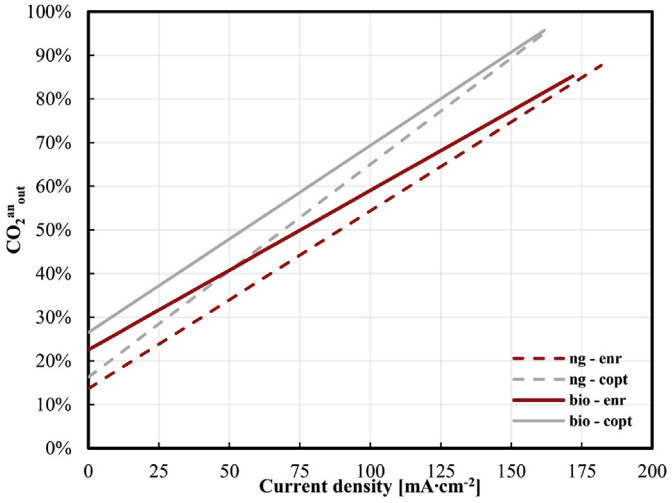

Fig. 5. Trend of the captured carbon dioxide from the MCFC and collected to the anodic exhaust for *enr* and *copt* cathode compositions. Note that at zero current density the curves with the same fuel compositions do not correspond because $CO^{an}_{2\ out}$ is a gas fraction. For readability *biopt* case, being very close to *enr*, is kept out from the plot.

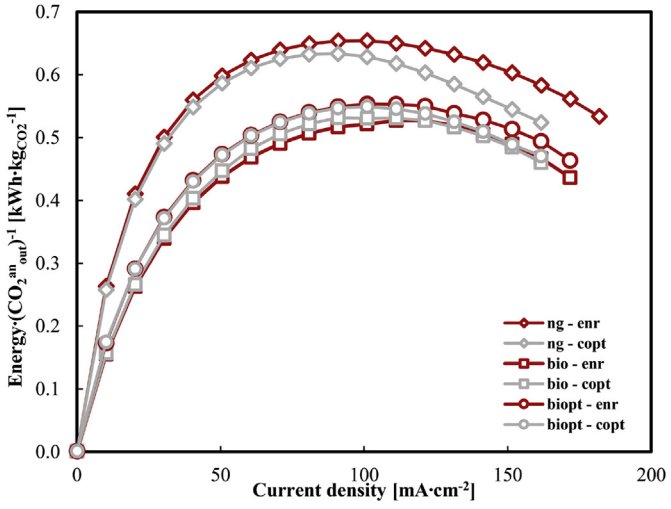

Fig. 6. Energy produced for *kg* of *captured* carbon dioxide.

from 90 to 110 $mA\ cm^{-2}$. It must be evidenced that, even if the energy produced per kg of $CO_{2\ out}^{an}$ allows comparing the MCFC with other CO_2 capture systems, at the same time it does not allow to choose optimal MCFC working conditions in CCS application, due to the trend of $CO_{2\ out}^{an}$.

To this regard, it's interesting to show the behavior of the efficiency as a function of the captured carbon dioxide $CO_{2\ out}^{an}$ (Fig. 7A): it's evident how the curves are grouped in two well defined families, depending on the cathode composition, with *copt* curves systematically shifted to the right side of the graph corresponding to higher percentages of captured CO_2. Obviously, this result is not true in terms of absolute captured CO_2, since *enr* compositions are able to reach higher current densities, which correspond to higher volumes of CO_2 removed from the cathode side. Regarding the fuel, for both families (cathode feeding conditions) from Fig. 7A it is evident that:

1. natural gas brings with itself less CO_2 so the relative curves start on the left of the corresponding ones obtained with biogas-like compositions;
2. over a certain value of current density, biogas is more efficient than natural gas. In particular, as previously seen the differences in η_e increases with current density, while the difference of the $CO_{2\ out}^{an}$ fraction decreases.

5. Performance of base CCS unit

5.1. System general features

The anode off-gas is mainly composed by carbon dioxide (up to 40%) and water (up to 55%) but also to a lesser extent of unused carbon monoxide and hydrogen (depending from the *fuel utilization*, around 10%). Before condensing water, the residual fuel should be removed, for example, through oxycombustion. In this occurrence, an oxycombustor must be added downstream the MCFC, together with an ASU used for oxygen separation which is calculated here assuming an electrical energy requirement of 0.295 $kWh \cdot kg_{O_2}^{-1}$ [27].

To go further in the present work, considering main outcomes of previous Section 4 and aiming to characterize the CCS application of MCFCs in the cases of feeding by natural gas and biogas, *ng-enr* and *bio-enr* cases are considered in the following for the analysis of the CCS section plant. To get a generalized result, such analysis is performed on the base CCS unit, already described in Section 2, installed downstream a power generation plant (ICE). Therefore, basing on the obtained results, a comparative analysis is carried out to evaluate the fuel effect on energy and CO_2 capture performance of the considered base CCS unit. Furthermore, to highlight improvements obtainable, specifically in terms of CO_2 performance under particular operating conditions, performance assessments by means of plant optimization are provided as example for the *biopt-copt* feeding conditions corresponding to the optimized layout proposed in Ref. [1].

Fig. 7B describes the electric efficiency trend, lowered by the ASU penalty, as a function of the overall carbon dioxide stored (i.e. the collected CO_2 from MCFC anode plus the CO converted by the ASU). The behavior does not change markedly respect to performance of the single MCFC shown in previous Fig. 7A. Obviously the introduction of this kind of design privileges high fuel utilization factors. Although the three solutions are just slightly different from this point of view, the efficiency loss for *bio-enr* is less than 5%, more than one percentage point better respect to the *ng* and the optimized (*biopt-copt* feeding) cases. The maximum $CO_{2\ storage}$ reaches 89.0% for natural gas and 86.5% for biogas, corresponding to specific absolute values of $2.02 \cdot 10^{-4}$ and $2.13 \cdot 10^{-4}\ kg_{CO_2} \cdot h^{-1} \cdot cm^{-2}$ respectively (Table 3). The *biopt-copt* case loses part of its advantage from a carbon capture point of view since all the curves result very tight. The impact of ASU contribution on the collected CO_2 is quite limited, while the fuel contribution is comparable with the carbon dioxide removed from the exhaust off-gas (particularly for the biogas-like fuel compositions). In the following, to produce data useful for the performance comparison of the base CCS unit for both natural gas and biogas feeding cases, two different sizing strategies are followed: parity of installed power of CCS base unit and parity of treated flowrate of exhaust gases from the topper plant. For both strategies, main unit features are provided in Section 5.2 to characterize energy and CO_2 performance under the different feeding conditions. These results are finally discussed in Section 5.3.

5.2. Retrofit base CCS unit sizing

On the basis of the experimental results already presented, it is possible to evaluate the size of a retrofit base CCS unit based on a MCFC stack. As already discussed, it includes the MCFC stack, fed by a reformer, and the oxycombustor-ASU for the final anodic off-gas treatment. It is remarked that, for a specific application, a retrofit plant must be sized basing on a complex framework including the total carbon dioxide flow delivered by the upstream power plant, specific country legislation on carbon dioxide emissions, carbon

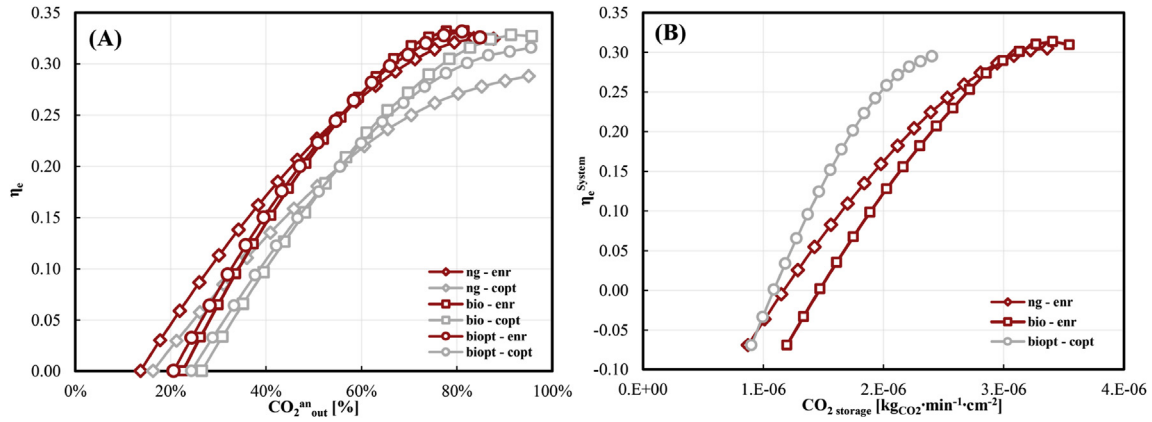

Fig. 7. (A) MCFC electric efficiency as a function of the *captured* carbon dioxide $CO_{2\ out}^{an}$; (B) electric efficiency as function of the *stored* carbon dioxide per minute and per specific MCFC area, in reference to the whole system.

Table 3
Specific absolute carbon dioxide flow rates separated and concentrated in the various steps (*removed*, an_{out} and *storage*, according to the nomenclature) of the MCFC + ASU system. Δ^{an}_{capt} [%] and $\Delta_{storage}$ [%] provide the carbon dioxide addition compared with the previous step, i.e. CO_2 contributions due to fuel (after reforming) and oxycombustion respectively.

		ng-enr	*biopt-copt*	*bio-enr*
$CO_{2\,rem}$	$[kg_{CO_2} \cdot h^{-1} \cdot cm^{-2}]$	$1.49 \cdot 10^{-4}$	$1.33 \cdot 10^{-4}$	$1.41 \cdot 10^{-4}$
$CO^{an}_{2\,out}$	$[kg_{CO_2} \cdot h^{-1} \cdot cm^{-2}]$	$1.95 \cdot 10^{-4}$	$1.99 \cdot 10^{-4}$	$2.08 \cdot 10^{-4}$
$CO_{2\,storage}$	$[kg_{CO_2} \cdot h^{-1} \cdot cm^{-2}]$	$2.02 \cdot 10^{-4}$	$2.04 \cdot 10^{-4}$	$2.13 \cdot 10^{-4}$
Δ^{an}_{out}	[%]	+30%	+50%	+48%
$\Delta_{storage}$	[%]	+3.55%	+2.82%	+2.23%

emission trading and fuel (whatever) availability/cost. Accordingly, a realistic sizing should be done to decrease the carbon emission to the lower allowed level (or as a function of possible penalization factors) by optimizing, as well as the plant size, the fraction of exhaust gas treated in order to take into account different and conflicting needs as:

- minimum capital cost by increasing the carbon capture capacity (i.e. $CO_{2\,rem}$) on the treated exhaust fraction;
- maximum MCFC electric efficiency (therefore the fuel exploitation) increasing the treated exhaust fraction (i.e. the overall cathodic inlet flow) with a consequent lower $CO_{2\,rem}$.

In the present work, aiming to characterize the CCS application of MCFCs in the cases of feeding by natural gas and biogas, obviously not all the aspects discussed above could be considered. Nevertheless, projecting the obtained results on the plant level, can better clarify MCFC and plant operating features, also as an effect of the conflicting criteria indicated above.

Therefore, according to the followed strategies, two different sizing processes were performed. The first one moves from a power request of 1 *MW* for repowering the host ICE plant. This value is a reference assumption coherent with the main generalized outcome aimed by the present work. The second strategy, instead, considers as initial assumption an exhaust CO_2 flowrate of $1,000\ kg_{CO_2} \cdot h^{-1}$ to be treated and delivered by the host plant. Main results are summarized in Tables 4 and 5, respectively. Capital cost was evaluated for all cases considering a specific cost of about 3,118 \$ m^{-2}, derived for the *ng* case (power of 1063 kW and total cells area 1023 m^2) assuming a cost of the MCFC system equal to 3,000 \$ kW^{-1} referred to the net power of the fuel cell [28]. The specific cost of the MCFC system includes, for simplicity, also the cost of the ASU and oxycombustor, whose sizes are proportional to the flow rate of residual fuel and oxidized compounds exiting the MCFC anode, which can be considered proportional to the MCFC power output.

Table 5
Main features of the base CCS unit, varying feeding conditions, sized to treat exhaust gases for a CO_2 flowrate of $1,000\ kg_{CO_2} \cdot h^{-1}$ delivered by the host plant.

Case		*ng-enr*	*biopt-copt*	*bio-enr*
Area	$[m^2]$	574	1015	574
η^{MCFC}_e	–	0.32	0.32	0.32
η^{System}_e	–	0.305	0.295	0.310
$\Delta\eta_e$	–	−6.0%	−6.5%	−4.7%
Fuel	$[kg\ kWh^{-1}]$	0.19	0.52	0.55
$CO_{2\,emitted}$	$[kg_{CO_2} \cdot h^{-1}]$	143	75	191
$CO_{2\,storage}$	$[kg_{CO_2} \cdot h^{-1}]$	1158	1464	1220
$CO_{2\,storage}$ (*)	[%]	89%	95.1%	86.5%
Power MCFC	[*kW*]	597	925	521
Power ASU	[*kW*]	36	59	25
Power CCS base Unit	[*kW*]	561	866	496
$En^{System} \cdot (CO_{2\,storage})^{-1}$	$[kWh \cdot kg^{-1}_{CO_2}]$	0.485	0.831	0.407
$Cost_{Capital}$	[\$]	1,790,000	3,160,000	1,790,000
$\Delta Cost_{Capital}$ (**)	[%]	–	+76.8%	−0.1%

(*) It is obtained as the ratio between the $CO_{2\,storage}$ and the CO_2 globally emitted from the system ($CO_{2\,storage} + CO_{2\,emitted}$).
(**) Referred to the *ng* case.

5.3. Performance discussion

5.3.1. Natural gas vs. biogas feeding

Natural gas feeding preserves the best performances of the base

Table 4
Main features of the base CCS unit, varying feeding conditions, sized to provide 1 *MW* for repowering the host plant.

Case		*ng-enr*	*biopt-copt*	*bio-enr*
Area	$[m^2]$	1023	1171	1155
η^{MCFC}_e	–	0.32	0.32	0.32
η^{System}_e	–	0.305	0.295	0.310
$\Delta\eta_e$	–	−6.0%	−6.5%	−4.7%
Fuel	$[kg\ kWh^{-1}]$	0.19	0.52	0.55
$CO_{2\,fuel}$	$[kg_{CO_2} \cdot h^{-1}]$	282	594	586
$CO_{2\,exhaust}$ (*)	$[kg_{CO_2} \cdot h^{-1}]$	1782	1154	2014
$CO_{2\,total\,inlet}$	$[kg_{CO_2} \cdot h^{-1}]$	2064	1749	2600
$CO_{2\,storage}$	$[kg_{CO_2} \cdot h^{-1}]$	2064	1690	2458
$CO_{2\,storage}$ (**)	[%]	89%	95.1%	86.5%
$CO_{2\,emitted}$ (*)	$[kg_{CO_2} \cdot h^{-1}]$	254	87	385
Power MCFC	[*kW*]	1063	1068	1049
Power ASU	[*kW*]	63	68	49
$En^{System} \cdot (CO_{2\,storage})^{-1}$	$[kWh \cdot kg^{-1}_{CO_2}]$	0.485	0.831	0.407
$Cost_{Capital}$	[\$]	3,190,000	3,650,000	3,600,000
$\Delta Cost_{Capital}$ (***)	[%]	–	+14.5%	+12.9%

(*) In the *biopt-copt* case, $CO_{2\,exhaust}$ and $CO_{2\,emitted}$ differ from $CO^{cath}_{2\,inlet}$ and $CO^{cath}_{2\,out}$ respectively, as a result of recirculation.
(**) It is obtained as the ratio between the $CO_{2\,storage}$ and the CO_2 globally delivered from the CCS base unit ($CO_{2\,storage} + CO_{2\,emitted}$).
(***) Referred to the *ng* case.

CCS unit under study, mainly in terms of power production. This feature allows to reduce capital cost, as evident in Table 4, when the plant layout is sized to fit the power demand. Changing the point of view, when a particular level of carbon capture is required, the operative cost due to an expensive and not renewable source, as natural gas, can be partially compensated by:

1. the extra power production ability, +10% compared with the biogas-like fuels (see Fig. 4A);
2. a lower capital cost, since the MCFC can run at higher current densities and more carbon dioxide is consequently removed (or a higher exhaust flow-rate can be treated).

According to the present experimentation, the second advantage is pretty limited (*ng-enr* shows +11% and +5.5% of extra carbon dioxide removed compared with, respectively, *bio-enr* and *biopt-copt*, Table 3) and totally lost (−1.4% and −5.4% on $CO_{2\ storage}$, Table 3) when also CO_2 derived from the fuel is taken into account. On the other hand, by increasing the cathodic flow, it's possible to increase the limit given by the use of carbon dioxide U_{CO_2} (Fig. 2C) to reach both higher current densities (that is higher level of $CO_{2\,rem}$) and power production, with the penalty of some percentage points in removed carbon dioxide.

Similarly to the case of natural gas feeding, even if slightly better, the electric efficiency of the MCFC fueled by biogas is penalized by the *CCS* configuration, that forces high cathodic carbon dioxide exploitation (U_{CO_2} between 80% and 90%), which corresponds to low fuel utilization.

Moreover, in the case of biogas feeding, it must be considered that biogas is a carbon dioxide carrier and this is critical for carbon capture performance of the base CCS unit. In this case, in fact, while MCFC is able to collect bigger absolute volume of CO_2 at the anodic off-gas, the relative amount of CO_2 stored is smaller than in the case of natural gas feeding. Evidently the excess of CO_2, contained in biogas, penalizes the overall performance, as well highlighted by the carbon dioxide content at the cathodic off-gas ($CO_{2\ emitted}$, Table 4). This is the biggest $CO_{2\ emitted}$ value among all investigated cases. Obviously, it must be considered that biogas is a renewable resource so that the carbon dioxide fraction can push towards *negative* emissions.

In details, regarding the first sizing strategy, relevant features of the base CCS unit, at parity of net installed power, are (Table 4):

- reduced MCFC total area for natural gas feeding (1,023 m^2 for *ng-enr* case vs. 1,155 m^2 for *bio-enr* case), leading to the lowest capital cost: biogas feeding implies an increase of about 13%;
- regarding CO_2 capture performance, a greater removal is performed in case of natural gas feeding. The CO_2 cathodic outlet stream (254 $kg_{CO_2} \cdot h^{-1}$) is reduced at 14% of the flowrate cathodic inlet (1, 782 $kg_{CO_2} \cdot h^{-1}$), while, in case of biogas feeding, it grows up to 19% of $CO_{2\ exhaust}$. In the same case, the increase of about 19% in total $CO_{2\ storage}$, shown in Table 4, is due to the biogas CO_2 content.

For what concerns the second sizing strategy (parity of CO_2 treated flowrate), it can be remarked that (Table 5):

- natural gas feeding exhibits higher CO_2 removal ability (similarly to the previous investigated strategy, at the cathode outlet only 14% of inlet CO_2 is present versus 19% for *bio-enr* case)
- similar features can be observed, for both natural gas and biogas feedings, in terms of total area and capital cost.
- different produced power values (597 *kW* and 521 *kW* for natural gas and biogas respectively) result for the same total area, with reduction of about 13% in *bio-enr* case.

5.3.2. System optimization: analysis of a specific case

The optimized configuration *biopt-copt* was defined to maximize CO_2 removal performance. As already discussed at single cell level, in fact, it reaches CO_2 removal and captured rates around 90% −95%, corresponding to a maximum $CO_{2\ storage}$ of 94.6% and a specific absolute value of $2.04 \cdot 10^{-4}$ $kg_{CO_2} \cdot h^{-1} \cdot cm^{-2}$ (Table 3), making the molten carbonate fuel cell comparable with the more efficient capture (but energy demanding) technologies. The slight electric efficiency reduction and the relative low overall power production are drawbacks. Furthermore, the main issue is the growth of the capital cost. In fact, mixture optimization is obtained by recirculating both cathodic (in the measure of 10%) and anodic (28.8%) off-gas flows to the cathodic inlet. Consequently, a reduced exhaust flowrate delivered by the topper plant can be treated for unitary MCFC area. This corresponds, making reference only to the CO_2 flowrate, to 35.2% and 42.6% of the CO_2 specific cathodic flow compared to *ng-enr* and *biogas-enr*, respectively. This produces an increase in cell area (about +76.7%) required to handle the same amount of flow delivered by a conventional plant.

With reference to main features resulting from CCS base unit sizing, for the optimized case, it can be highlighted (Tables 4 and 5):

- the largest overall area (for both sizing strategies), leading to the highest capital cost. In particular, assuming a constant requested installed power, an increase of 14.5% arises; while, keeping the same treated flowrate, capital cost is 76.8% the one estimated for the *ng-enr* case. It must be evidenced that, according to the latter sizing strategy, net installed power increases of about 54% respect to *ng-enr* case.
- the highest CO_2 capture performance in reference to the CO_2 cathodic outlet stream. In fact, it decreases to 9% of the flowrate cathodic inlet, vs. 14% and 19% resulting for *ng-enr* and *biogas-enr*, respectively.
- a slight reduction in overall efficiency (about 1% point with respect to *ng-enr* case).

6. Conclusions

The present work provided an analysis of a CCS unit, constituted by a MCFC stack integrated with oxycombustor-ASU and directly fed through a reformer, intended for the application to carbon capture downstream a reciprocating internal combustion engine in a wastewater treatment plant. Specifically, a comparative analysis, considering feeding by biogas or natural gas to the MCFC, is carried out to evaluate the fuel effect on energy and CO_2 capture performance of the considered base CCS unit, as well as on its sizing and cost. All evaluations are based on the outcomes of a specific experimental activity performed at the Fuel Cell Laboratory of University of Perugia.

A preliminary techno-economic evaluation, developed for the more interesting case studies, were provided by assuming two alternative design criteria: constant installed MCFC electric power and constant exhausts flowrate to be treated.

Main findings are:

i the ability of the MCFC-CCS base unit to store 89% to 86% of the treated carbon dioxide, respectively in the case of feeding the fuel cell with natural gas or biogas;
ii specific energy production of 0.485 *kWh* and 0.485 *kWh* per *kg* of stored CO_2, respectively for the former and the latter solution. Moreover, the impact of the MCFC capital cost on the competitiveness of this kind of installation is remarked.

As a general result of the comparative analysis, at constant installed electric MCFC power, biogas feeding results in a higher

MCFC total area with an increase of about 13% in capital cost of the base CCS unit. Also CO_2 capture performance is slightly lower. The CO_2 cathodic outlet stream, in fact, in the case of natural gas feeding is equal to 14% of the flowrate cathodic inlet, while in case of biogas feeding grows up to 19% of treated CO_2. Also at constant CO_2 treated flowrate, natural gas feeding exhibits higher CO_2 removal ability, similarly to the previous investigated strategy, bringing about an increment of 13% in produced net power (561 *kW* vs. 496 *kW*) for the same MCFC area and capital cost.

An additional optimized configuration (*biopt-copt*) fueled by biogas was investigated. In this case 95% of treated CO_2 is stored, making the molten carbonate fuel cell comparable with the more efficient capture (but energy demanding) technologies. Disadvantages, with respect to not-optimized solutions, are the slight electric efficiency reduction, the relative low overall power production and, mainly, the significant capital cost growth (+14.5% and about +76.7% at constant installed power and at constant treated flowrate, respectively).

Further investigation of possible biogas sources and alternative uses (biogas could be exploited in the ICE and a related loss in energy production could arise due to possible differences in conversion efficiency) must be performed in the future to provide a comparative profitability analysis of the CCS base units powered by natural gas and biogas respectively. Also a complete LCA (*Life Cycle Assessment*) of the CO_2 cycle will be assessed to provide a comprehensive assessment of the different solutions eco-efficiency.

Acknowledgments

The work was partly supported by H2FC European Infrastructure Project (Integrating European Infrastructure to support science and development of Hydrogen and Fuel Cell Technologies towards European Strategy for Sustainable Competitive and Secure Energy) Theme [INFRA-2011-1.1.16.], Grant agreement 284522.

References

[1] D. Sánchez, B. Monje, R. Chacartegui, S. Campanari, Potential of molten carbonate fuel cells to enhance the performance of CHP plants in sewage treatment facilities, Int. J. Hydrogen Energy 38 (1) (2013) 394–405, http://dx.doi.org/10.1016/j.ijhydene.2012.09.145. URL, http://linkinghub.elsevier.com/retrieve/pii/S0360319912022124.

[2] J. Milewski, J. Lewandowski, Separating CO2 from flue gases using a molten carbonate fuel cell, IERI Procedia 1 (48) (2012) 232–237, http://dx.doi.org/10.1016/j.ieri.2012.06.036. URL, http://linkinghub.elsevier.com/retrieve/pii/S2212667812000378.

[3] S. Campanari, Carbon dioxide separation from high temperature fuel cell power plants, J. Power Sources 112 (1) (2002) 273–289, http://dx.doi.org/10.1016/S0378-7753(02)00395-6. URL, http://linkinghub.elsevier.com/retrieve/pii/S0378775302003956.

[4] A. Amorelli, M. Wilkinson, P. Bedont, P. Capobianco, B. Marcenaro, F. Parodi, A. Torazza, An experimental investigation into the use of molten carbonate fuel cells to capture CO2 from gas turbine exhaust gases, Energy 29 (9–10) (2004) 1279–1284, http://dx.doi.org/10.1016/j.energy.2004.03.087. URL, http://linkinghub.elsevier.com/retrieve/pii/S0360544204001707.

[5] U. Desideri, S. Proietti, P. Sdringola, G. Cinti, F. Curbis, MCFC-based CO2 capture system for small scale CHP plants, Int. J. Hydrogen Energy 37 (24) (2012) 19295–19303, http://dx.doi.org/10.1016/j.ijhydene.2012.05.048. URL, http://dx.doi.org/10.1016/j.ijhydene.2012.05.048, http://linkinghub.elsevier.com/retrieve/pii/S0360319912011913.

[6] J. Milewski, W. Bujalski, M. Woowicz, K. Futyma, J. Kucowski, R. Bernat, Experimental investigation of CO2 separation from lignite flue gases by 100 cm2 single Molten Carbonate Fuel Cell, Int. J. Hydrogen Energy 39 (3) (2014) 1558–1563, http://dx.doi.org/10.1016/j.ijhydene.2013.08.144. URL, http://dx.doi.org/10.1016/j.ijhydene.2013.08.144, http://linkinghub.elsevier.com/retrieve/pii/S0360319913021939.

[7] K. Sugiura, K. Takei, K. Tanimoto, Y. Miyazaki, The carbon dioxide concentrator by using MCFC, J. Power Sources 118 (1–2) (2003) 218–227, http://dx.doi.org/10.1016/S0378-7753(03)00084-3. URL, http://dx.doi.org/10.1016/S0378-7753(03)00084-3.

[8] G. Discepoli, G. Cinti, U. Desideri, D. Penchini, S. Proietti, Carbon capture with molten carbonate fuel cells: experimental tests and fuel cell performance assessment, Int. J. Greenh. Gas Control 9 (2012) 372–384, http://dx.doi.org/10.1016/j.ijggc.2012.05.002. URL, http://dx.doi.org/10.1016/j.ijggc.2012.05.002, http://linkinghub.elsevier.com/retrieve/pii/S1750583612001053.

[9] I. Rexed, M. Della Pietra, S.J. McPhail, G. Lindbergh, C. Lagergren, Molten carbonate fuel cells for CO2 separation and segregation by retrofitting existing plants an analysis of feasible operating windows and first experimental findings, Int. J. Greenh. Gas Control 35 (2015) 120–130, http://dx.doi.org/10.1016/j.ijggc.2015.01.012. URL, http://linkinghub.elsevier.com/retrieve/pii/S1750583615000286.

[10] Www.fuelcells.org/wp-content/uploads/2012/02/TulareCaseStudy.pdf, Fuel Cell System Turns Waste into Electricity at the Tulare Wastewater Treatment Plant, 2007. URL, www.fuelcells.org/wp-content/uploads/2012/02/TulareCaseStudy.pdf\newobj(a)newobj(E)newobj(Z).

[11] A. Buonomano, F. Calise, G. Ferruzzi, A. Palombo, Molten carbonate fuel cell: an experimental analysis of a 1kW system fed by landfill gas, Appl. Energy 140 (2015) 146–160, http://dx.doi.org/10.1016/j.apenergy.2014.11.044. URL, http://linkinghub.elsevier.com/retrieve/pii/S0306261914012136.

[12] S. Trogisch, J. Hoffmann, L. Daza Bertrand, Operation of molten carbonate fuel cells with different biogas sources: a challenging approach for field trials, J. Power Sources 145 (2) (2005) 632–638, http://dx.doi.org/10.1016/j.jpowsour.2005.02.053. URL, http://linkinghub.elsevier.com/retrieve/pii/S0378775305002703.

[13] E. Sisani, G. Cinti, G. Discepoli, D. Penchini, U. Desideri, F. Marmottini, Adsorptive removal of H2S in biogas conditions for high temperature fuel cell systems, Int. J. Hydrogen Energy 39 (36) (2014) 21753–21766, http://dx.doi.org/10.1016/j.ijhydene.2014.07.173. URL, http://dx.doi.org/10.1016/j.ijhydene.2014.07.173, http://linkinghub.elsevier.com/retrieve/pii/S0360319914022198.

[14] U. Desideri, S. Proietti, G. Cinti, P. Sdringola, C. Rossi, Analysis of pollutant emissions from cogeneration and district heating systems aimed to a feasibility study of MCFC technology for carbon dioxide separation as retrofitting of existing plants, Int. J. Greenh. Gas Control 5 (6) (2011) 1663–1673, http://dx.doi.org/10.1016/j.ijggc.2011.10.001. URL, http://linkinghub.elsevier.com/retrieve/pii/S1750583611001836.

[15] F. Zaza, C. Paoletti, R. Lo Presti, E. Simonetti, M. Pasquali, Bioenergy from fuel cell: effects of hydrogen sulfide impurities on performance of MCFC fed with biogas, in: Fundamentals and Developments of Fuel Cells Conference - FDFC2008, ENEA, 2008. URL, http://perso.ensem.inpl-nancy.fr/Olivier.Lottin/FDFC08/CD/Contributions/FCHZAZA30-0967M.pdf.

[16] V. Cigolotti, S.J. McPhail, A. Moreno, S.P. Yoon, J.H. Han, S.W. Nam, T.-H. Lim, MCFC fed with biogas: experimental investigation of sulphur poisoning using impedance spectroscopy, Int. J. Hydrogen Energy 36 (16) (2011) 10311–10318, http://dx.doi.org/10.1016/j.ijhydene.2010.09.100. URL, http://linkinghub.elsevier.com/retrieve/pii/S0360319910020100.

[17] I. Rexed, C. Lagergren, G. Lindbergh, Effect of sulfur contaminants on MCFC performance, Int. J. Hydrogen Energy 39 (23) (2014) 12242–12250, http://dx.doi.org/10.1016/j.ijhydene.2014.03.068. URL, http://linkinghub.elsevier.com/retrieve/pii/S0360319914007241.

[18] N. Di Giulio, B. Bosio, J. Han, S.J. McPhail, Experimental analysis of SO2 effects on molten carbonate fuel cells, Int. J. Hydrogen Energy 39 (23) (2014) 12300–12308, http://dx.doi.org/10.1016/j.ijhydene.2014.04.120. URL, http://linkinghub.elsevier.com/retrieve/pii/S0360319914011781.

[19] N. Di Giulio, B. Bosio, V. Cigolotti, S. Nam, Experimental and theoretical analysis of H2S effects on MCFCs, Int. J. Hydrogen Energy 37 (24) (2012) 19329–19336, http://dx.doi.org/10.1016/j.ijhydene.2012.03.086. URL, http://linkinghub.elsevier.com/retrieve/pii/S0360319912007331.

[20] K. Gharieh, M.A. Jafari, Q. Guo, Investment in hydrogen tri-generation for wastewater treatment plants under uncertainties, J. Power Sources 297 (2015) 302–314, http://dx.doi.org/10.1016/j.jpowsour.2015.07.093. URL, http://linkinghub.elsevier.com/retrieve/pii/S0378775315301439.

[21] N. de Arespacochaga, C. Valderrama, C. Peregrina, A. Hornero, L. Bouchy, J. Cortina, On-site cogeneration with sewage biogas via high-temperature fuel cells: benchmarking against other options based on industrial-scale data, Fuel Process. Technol. (2015), http://dx.doi.org/10.1016/j.fuproc.2015.07.006. URL, http://linkinghub.elsevier.com/retrieve/pii/S0378382015300837.

[22] G. Rinaldi, D. McLarty, J. Brouwer, A. Lanzini, M. Santarelli, Study of CO2 recovery in a carbonate fuel cell tri-generation plant, J. Power Sources 284 (2015) 16–26, http://dx.doi.org/10.1016/j.jpowsour.2015.02.147. URL, http://linkinghub.elsevier.com/retrieve/pii/S0378775315003936.

[23] H. Huang, J. Li, Z. He, T. Zeng, N. Kobayashi, M. Kubota, Performance analysis of a MCFC/MGT hybrid power system Bi-Fueled by city gas and biogas, Energies 8 (6) (2015) 5661–5677, http://dx.doi.org/10.3390/en8065661. URL, http://www.mdpi.com/1996-1073/8/6/5661/.

[24] H. Kasai, T. Matsuo, M. Hosaka, N. Motohira, N. Kamiya, K. Ota, High temperature electrochemical separation of carbon dioxide using molten carbonate, DENKI KAGAKU 66 (6) (1998) 635–640.

[25] C.-G. Lee, K.-S. Ahn, H.-C. Lim, J.-M. Oh, Effect of carbon monoxide addition to the anode of a molten carbonate fuel cell, J. Power Sources 125 (2) (2004) 166–171, http://dx.doi.org/10.1016/j.jpowsour.2003.07.014. URL, http://linkinghub.elsevier.com/retrieve/pii/S0378775303008498.

[26] J. Milewski, G. Discepoli, U. Desideri, Modeling the performance of MCFC for various fuel and oxidant compositions, Int. J. Hydrogen Energy 39 (22) (2014) 11713–11721, http://dx.doi.org/10.1016/j.ijhydene.2014.05.151. URL, http://linkinghub.elsevier.com/retrieve/pii/S0360319914015638.

[27] W. Castle, Air Separation and Liquefaction: Recent Developments and Prospects for the Beginning of the New Millennium, 2002, http://dx.doi.org/

10.1016/S0140-7007(01)00003-2.
[28] S. Campanari, P. Chiesa, G. Manzolini, S. Bedogni, Economic analysis of CO2 capture from natural gas combined cycles using Molten Carbonate Fuel Cells, Appl. Energy 130 (2014) 562–573, http://dx.doi.org/10.1016/j.apenergy.2014.04.011. URL, http://dx.doi.org/10.1016/j.apenergy.2014.04.011, http://linkinghub.elsevier.com/retrieve/pii/S0306261914003547.

Nomenclature

ASU: Air Separation Unit
$CO_{2\,exhaust}$: CO_2 content in the exhaust gases to be treated
$CO_{2\ inlet}^{cath}$: CO_2 content in the cathodic inlet stream, CO_2 content in the cathodic outlet stream
$CO_{2\,fuel}$: CO_2 content in the fuel mixture at the anode inlet
$CO_{2\,rem}$: CO_2 removed from cathode
$CO_{2\ out}^{an}$: CO_2 content in the anodic off-gases
$CO_{2\ in}^{oxy}$: CO_2 content in the ASU inlet stream
CO_2^{CO}: CO_2 produced by the *CO* oxycombustion
$CO_{2\,storage}$: CO_2 content at the oxycombustor outlet
$CO_{2\,emitted}$: CO_2 residual content in the treated gases downstream the cathode outlet
DC: Direct Current
$En^{System}{\cdot}(CO_{2\,storage})^{-1}$: Energy produced by the CCS base unit for *kg* of CO_2 stored
η_e^{MCFC}: MCFC unit efficiency
η_e^{System}: CCS base unit efficiency
$\Delta\eta_e$: $\eta_e^{MCFC} - \eta_e^{System}$
H_2^{eq}: Equivalent Hydrogen Flow rate
ICE: Internal Combustion Engine
m_{H_2}: H_2 molar flow rate in the fuel
m_{CO}: *CO* molar flow rate in the fuel
m_{CH_4}: CH_4 molar flow rate in the fuel
MCFC: Molten Carbonate Fuel Cell
X_{CO}: *CO* molar fraction
X_{CO_2}: CO_2 molar fraction
X_{H_2}: H_2 molar fraction
X_{H_2O}: H_2O molar fraction
X_{N_2}: N_2 molar fraction